Online Monitoring of Marine Turbine Insulation Condition Based on High Frequency Models - Methodology for finding the " best " identification protocol

Esseddik Ferdjallah-Kherkhachi, Emmanuel Schaeffer, Luc Loron, Mohamed Benbouzid

Online Monitoring of Marine Turbine Insulation Condition Based on High Frequency Models

Methodology for finding the "best" identification protocol

E. Ferdjallah-kh, E. Schaeffer, L. Loron
University of Nantes, EA 4642 IREENA
Saint-Nazaire, France
esseddik.ferdjallah-kherkhachi@univ-nantes.fr
emmanuel.schaeffer@univ-nantes.fr
luc.loron@univ-nantes.fr

M.E.H. Benbouzid
University of Brest, EA 4325 LBMS
Brest, France
Mohamed.Benbouzid@univ-brest.fr

***Abstract*— This paper investigates the online monitoring of electrical machine winding insulation systems based on parametric modeling and identification. The proposed method consists in monitoring the drift of diagnostic indicators built from in-situ estimation of high-frequency electrical model parameters. The involved model structures are derived from the RLC network modeling of the winding insulation, with more or less lumped parameters. Because they often present an important modeling noise, the authors propose to use the output error method not only to estimate the model parameter values but also to evaluate their uncertainty. This process is based on the numerical integration of the model sensitivity functions. The so-called global identification scheme is coupled with an optimization algorithm that brings the closer combination of any diagnostic model structure and its excitation protocol usable in operating conditions. Experimental data recorded from an industrial wound machines are used to illustrate the methodology.**

Keywords—Fault diagnosis,condition monitoring, aging, insulation, stator winding, marine renewable energy, parametric identification.

I. INTRODUCTION

Among the various ocean energy technologies under development, tidal stream and offshore wind turbines have nowadays reached their demonstration or even commercial size. However, their first operating feedbacks and also recent research reports on Marine Renewable Energy (MRE) have highlighted the complexity and the harshness of the marine environment [1],[2]. Thus, the reduction of the capital expenditure and the operating costs of the offshore energy farms are clearly the technological and scientific barriers that should be unlocked to ensure the economical viability of the MRE [3].

To this end, the predictive maintenance is a key issue [4]. Indeed, due to the cyclical nature of marine energy resources, the insulation system of marine electrical generators suffers regular thermal cycling and is therefore hardly stressed [2]. To avoid its premature degradation by thermal, mechanical (lamination) or chemical processes that could leads to an unscheduled costly outage, the most efficient way is to continuously monitor the insulation health state. It is well known that the aging of an insulation system mainly results in the variation of its capacitance and resistance: this is the underlying principle of the classical offline diagnostic methods such as RI and PI [5][6]. For the online monitoring of stator insulation condition, the Partial Discharge (PD) analysis is currently the only mature technology [4] But it may present serious limits for in-situ monitoring when the measurements of the partial discharges are done in a noisy environment. The analysis of the leakage currents [7] or the detection of resonance frequency changes by measurement of high frequency electrical field changes [8] are some alternative methods proposed in recent scientific literature.

The in-situ monitoring approach investigated in this paper is based on the online estimation of turn-to-turn and turn-to-ground capacitances of electrical parametric models [9][10]. The drift of their estimated values can be used for planning optimized corrective maintenance. Indeed, previous researche shows that the winding must be changed when the capacitance increase of 10 % [11]. Nevertheless, taking the right decision required not only to link the model parameter shifts to the physical aging phenomena , but also to evaluate the confidence in the estimated values in order to avoid false alarms. This is the subject of this article. First, the principle of the proposed diagnostic approach is justified from the predictive maintenance context of offshore marine turbines. The theoretical framework of model identification by the output error method is presented in the next part. The third section illustrate the methodology with experimental data.

II. MATERIAL AND METHOD

A. System modeling

Modeling and identification are essential stages for system control, optimal design and monitoring. Discrete recurrence equations and identification algorithms derived from the least square framework are often used for the synthesis of control laws [12]. But if the goal is to deeply understand the system behavior, then the approach using knowledge continuous-time models is preferable. Indeed, their parameters have a physical signification and can be more simply linked to the physical phenomena taking place in the system to monitor [10].

This *a priori* knowledge allows not only the experimenter to propose different sets of mathematical equations – also

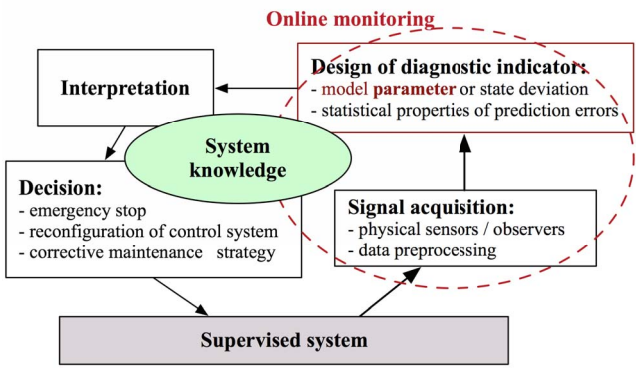

Fig. 1. Importance of knowledge in the maintenance scheme

called model structures – close to the physical nature of the system, but also to build diagnostic indicators and to interpret their drift for making strategicdecision. Fig. 1 shows the central role of knowledge in any predictive maintenance scheme [13]. The interpretation and decision algorithms are not in the scope of this work. The present study only focuses on the indicator design with estimated parameters of model structures given by the following state-space representation:

$$M(\boldsymbol{\theta}):\begin{cases}\dot{\boldsymbol{x}}(t,\boldsymbol{\theta}) = \boldsymbol{f}\big(\boldsymbol{x}(t,\boldsymbol{\theta}),\boldsymbol{\theta},u(t)\big)\\ y_m(t,\boldsymbol{\theta}) = g\big(\boldsymbol{x}(t,\boldsymbol{\theta}),\boldsymbol{\theta},u(t)\big)\end{cases} \quad (1)$$

where $\boldsymbol{\theta}$ is the parameter vector, $\boldsymbol{x}(t,\boldsymbol{\theta})$ is the state-vector, the input *u(t)* and the model output $y_m(t,\boldsymbol{\theta})$ can be scalar or vector, and the functions $\boldsymbol{f}$and g are based on physical laws which are generally non-linear with respect to parameters. Note that bold letters refer to vectors.

In practical terms, the function $\boldsymbol{f}$ and g are derived from the classical modeling approach of transformer and electrical machine winding [14]. They can deal with very simple models, such as three *R, L, C* lumped elements in series, or more complex network that can explain the propagation of the voltage in the insulation system. In fact, choosing a model structure to investigate remains a difficult initial phase where the experience of the user and its understanding of physical phenomena remain a key condition of the success. In what concerns us,it is well-known that the winding conductor resistance depends on temperatur (T°) and that the capacitance of a dielectric element change with aging as well as with moisture, and to a lesser extent with T° [4]. Moreover, the inductance parameter of a winding conductor elementary volume deals with the energy localized in the circuit flowed by the electromagnetic field, which remains confined in the slot at high frequency[15]. Previous studieshave shown that the self and mutual inductance can be considered constant in the frequency range [200 kHz - 100 MHz][16].

These kind of considerations may allow to reduce the number of unknown model parametersthat must be online estimated for insulation diagnosis. For example, the self and mutual inductances of a winding distributed constant model do not depend on insulation aging, moisture anf T°. In the insulation diagnostic context, they can be initialized by finite element method or global identification methods such as the genetic algorithms.

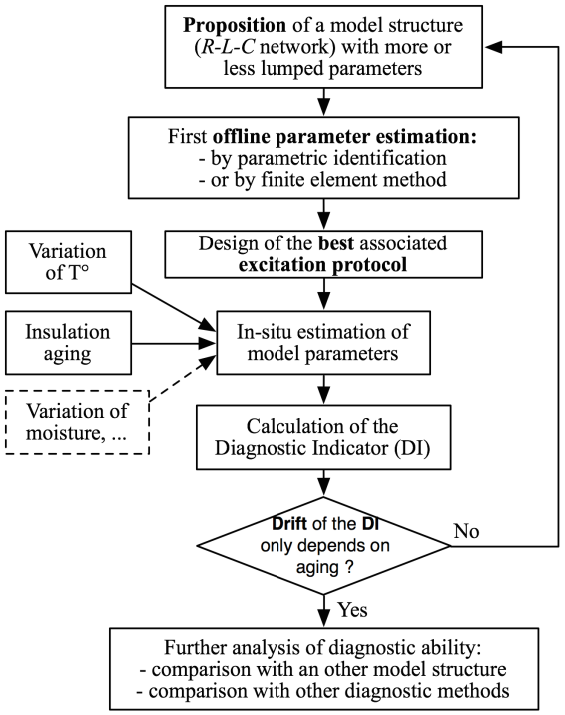

Fig. 2. Scheme of model research.

It is no longer true for too lumped constant models such the one used in section III (Fig.11) to illustrate the optimization of excitation protocol. The search of a "good" diagnostic model should therefore tend to increase the fineness of the model, *i.e.* to decrease the size of the elementary physical volumes modeled by lumped *R, L, C* elements. This model fineness is related to the dimension of the state vector of (1), and as consequence to its simulation cost. On the other hand, the next parts will explain that the more model parameters, the more the excitation protocol must provide power in a wide frequency range, and the more parameter uncertaintiesare likely to increase.

In other terms, the diagnostic model must present the best tradeoff bewteen fineness of the model structure and the

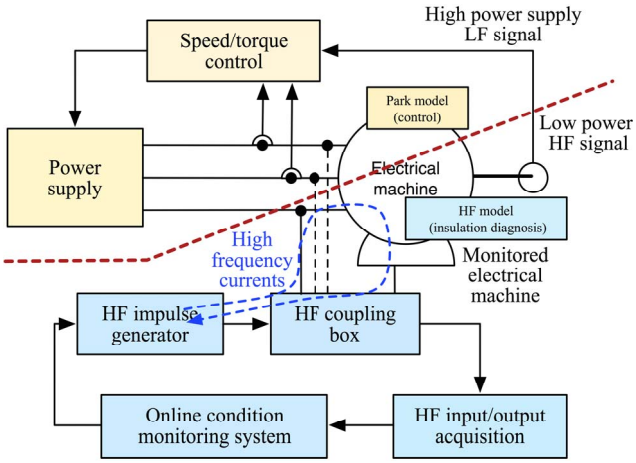

Fig. 3. Online insulation system excitation

number of its physical parameters. Fig. 2 resumes the process of system modelling dedicated to in-situ insulation diagnosis. In this scheme, the parameter estimation must be done with respect to industrial constraints; in particularly the excitation of the electrical machine insulation system should not disturb the variable speed drive.

B. Principle of system excitation and measurements

As explained below, the model identifiability is closely related to the excitation signal that can be used for system identification. Fig. 3 shows the technical solution carried out for the in-situ excitation of the insulation system. The monitored generator is torque-controlled in a closed-loop drive. But the high frequency excitation is applied to the generator insulation through a coupling box, between one or several phases and the stator housing. Therefore, the system identification is performed in a open-loop context, and do not required specific algorithms [17].

A high-frequency high-voltage signal generator has been specially developed for testing different excitation protocols (further studies will also explore the feasibility of using the high frequency spectral content of the PWM inverter supply). The pulse generator is based on a Mosfet half bridge with a close driver system that controls the transistor switches with a very low match delay so that the rising and falling rates of the voltage impulses reach approximately *10 V/ns*. The half bridge is driven by a microcontroller card, which simplifies the design of different excitation protocols, from the simple step up to the pseudo random binary signal (Fig. 4). The coupling box contains two capacitances C_p which value is very higher than the ones of the *R-L-C* network models (typically several *nF*). Their impedance can therefore be neglected in the high frequency range of the input/output signals used for the insulation system identification. The resistance R_d ensures the impedance adaptation of the BNC cable and R_m is used as sensor for the measurement of the high frequency current flowing in the insulation system. The input system $u = V_2$ and its currentoutput $y_s = (V_1 - V_2)/R_m$ are acquired by a oscilloscope Yokogawa DL9140, equipped with a 8 bits AD converter rating at 2.5 GHz. The experimental bench used for illustating the methodology is presented in section III.

C. System identification by the output error method

Many identification algorithms can be used for system identification. The choice depends on the nature of the model structure (linear or not with respect to the parameters and/or to the inputs), the nature of the measurement and structure noises, the dynamic of the physical changes to diagnose, or even the acceptable computational cost [18], [19], [20].

In fact, the insulation system aging has a dynamic of several years and the calculation cost of a MRE turbine monitoring system is clearly not a criterion compared to the economic and industrial strakes of their maintenance. Moreover, the outputs of continuous-time models derived from *R-L-C* networks are not linear in respect to their parameters. Thus, we propose to use the output error method and the sensitivity functions for insulation system identification [21]. This method presents a computational cost much higher than methods derived from least-squares but it provides an unbiased estimator with a relative immunity in respect to modeling errors [17]. This is an interesting feature because the required simplicity of the diagnostic model generally leads to an important modeling noise.

Fig 5 resumes the underlying principle of the output error method for an output error model: the system output $y_s(t)$ is considered as the sum of the model output for the right value of parameter $\boldsymbol{\theta}^*$ and an output noise $b(t)$ which embeds measurement and modeling noise. Let $\boldsymbol{\theta}$ be an estimation of $\boldsymbol{\theta}^*$. Then, a simulation of the system output $y_m(t, \boldsymbol{\theta})$ using only the measured input signal $u(t)$ can be obtained by the numerical integration of the continuous state-space model defined by (1). It can be performed by using the exponential matrix in case of linear state-space or the *Runge Kutta 4* algorithm in more general case. Then, the optimal estimated parameter vector $\boldsymbol{\theta_o}$ is obtained by the minimization of the following quadratic criterion $D(\boldsymbol{\theta})$, also called the state-distance[22]:

$$D(\boldsymbol{\theta}) = \sum_{k=1}^{N} \boldsymbol{e}(k, \boldsymbol{\theta})^T \boldsymbol{e}(k, \boldsymbol{\theta}) \quad (2)$$

$$\boldsymbol{\theta}_o = \arg\min D(\boldsymbol{\theta}) \quad (3)$$

where N is the number of input samples and $e(k, \boldsymbol{\theta}) = y_s(k) - y_m(k, \boldsymbol{\theta})$ is the output error at sample time t_k, which can be a scalar or a vector depending on the dimension of the system output. Many methods can be used for the non-linear optimization of the multivariable function $D(\boldsymbol{\theta})$. Each of them has its own advantages and drawbacks. For example the Nelder-Mead algorithm [23] ensures the convergence robustness even with a bad initialization, whereas the gradient algorithms ensure a small convergence time near the optimum[21]. As previously said, an offline method can perform an initial global optimum usable for a gradient

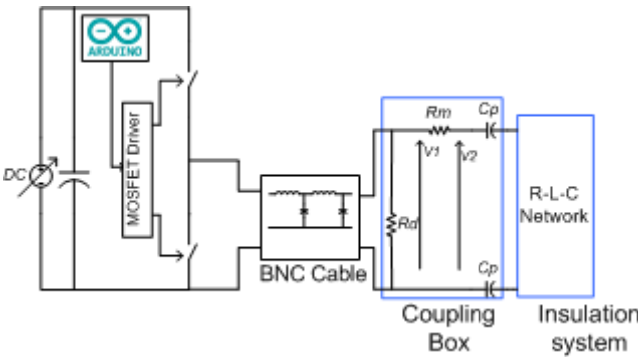

Fig. 4. Online excitation of the winding insulation system.

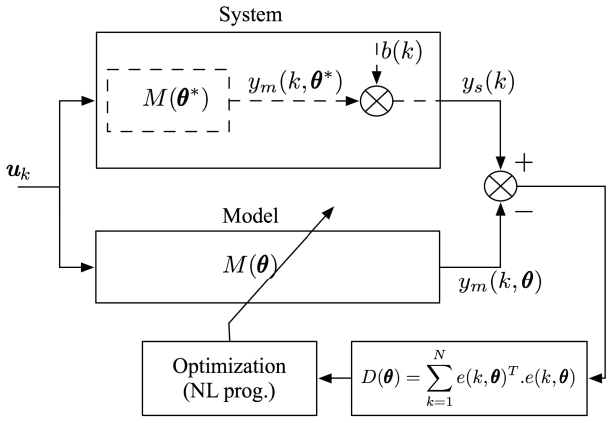

Fig. 5. Principle of the output error method (with the OE model).

method. And the dynamic of the insulation aging and thermal phenomena are very slow. Therefore the gradient algorithms are well adapted to the problematic of model-based online monitoring of insulation system.

Near the optimum, $\boldsymbol{\theta} = \boldsymbol{\theta}_o + \delta\boldsymbol{\theta}$ and the Taylor expansion of the state-distance gives:

$$D(\boldsymbol{\theta}) \approx D(\boldsymbol{\theta}_o) + \delta\boldsymbol{\theta}^T.\underbrace{\boldsymbol{G}(\boldsymbol{\theta}_o)}_{=0} + \frac{1}{2}\delta\boldsymbol{\theta}^T.\mathcal{H}(\boldsymbol{\theta}_o).\delta\boldsymbol{\theta} \quad (4)$$

where $\boldsymbol{G}(\boldsymbol{\theta}_o)$ and $\mathcal{H}(\boldsymbol{\theta}_o)$ denote the gradient and the hessian of D at point $\boldsymbol{\theta}_o$. Then, the derivative of (4) with respect to $\boldsymbol{\theta}$ gives:

$$\boldsymbol{G}(\boldsymbol{\theta}) = \mathcal{H}(\boldsymbol{\theta}_o)(\boldsymbol{\theta} - \boldsymbol{\theta}_o) \quad (5)$$

that should allows to reach the objective point $\boldsymbol{\theta}_o$ in one iteration from the starting point $\boldsymbol{\theta}$. Unfortunately, (4) is an approximation of the hyper-surface $D(\boldsymbol{\theta})$ near the objective point, and therefore multiple iterations are required. One can for example use the Newton algorithm [24]:

$$\boldsymbol{\theta}^{n+1} = \boldsymbol{\theta}^n + \lambda.(\mathcal{H}(\boldsymbol{\theta}^n)^{-1}.\boldsymbol{G}(\boldsymbol{\theta}^n) \quad (6)$$

for which the gradient vector $\boldsymbol{G}(\boldsymbol{\theta}^n)$ gives the direction of the search in the parametric space, whereas the inverse of the hessian matrix gives the depth of the descent. In practice, the algorithm must be supervised by a control parameter λ initialized to the unit at each nth iteration and that can be decreased in order to ensure that $D(\boldsymbol{\theta}^{n+1}) \leq D(\boldsymbol{\theta}^n)$. Moreover, the numerical derivation of $D(\boldsymbol{\theta})$ for the calculation of $\mathcal{H}$ and $\boldsymbol{G}$ will induce dramatically computational problems. A better solution consists in using the sensitivity functions. Indeed, by derivating (2) two times in respect to $\boldsymbol{\theta}$ one obtains the following gradient and hessian expressions, which only depend on the measurements, the model simulated output and the values of the output-sensitivity functions:

$$\boldsymbol{G}(\boldsymbol{\theta}) = -2\sum_{k=1}^{N}\psi(k,\boldsymbol{\theta})^T.\boldsymbol{e}(k,\boldsymbol{\theta}) \quad (7)$$

$$\mathcal{H}(\boldsymbol{\theta}) \simeq 2\sum_{k=1}^{N}\psi(k,\boldsymbol{\theta})^T.\psi(k,\boldsymbol{\theta}) \quad (8)$$

where $\psi(k,\boldsymbol{\theta}) = \left[\sigma_{i,\theta_j}(k,\boldsymbol{\theta})\right]$ is the jacobian matrix of $y_m(k,\boldsymbol{\theta})$ and the output-sensibility function $\sigma_{i,\theta_j}(k,\boldsymbol{\theta})$evaluate the sensibility of the ith model output in respect to the jth parameter θ_j. Note that $\psi(k,\boldsymbol{\theta})$ is a single-row matrix if the model output is scalar. Equation (7) shows that the jth gradient component $\partial D(\boldsymbol{\theta})/\partial\theta_j$ (giving the search direction in the θ_j-axis) deals with the sum of the output errors weighted by the output-sensitivity function of the parameter θ_j. Indeed, the output errors at each sample time can be all the more reduced by a small variation $\partial\theta_j$ than the model output is sensible to this parameter. In fact, equation (8) proposes an approximation of the hessian matrix by neglecting the second order derivatives of the model output. This approximation ensures the pseudo-hessian $\mathcal{H}(\boldsymbol{\theta})$ defined by (8) to be a positive definite matrix. In other words, the hyper-surface $D(\boldsymbol{\theta})$ is approximated at each nth iteration step of (6) by the hyper-ellipsoïd $S_{\boldsymbol{\theta}^n}(\boldsymbol{\theta})$ given by:

$$S_{\boldsymbol{\theta}^n}(\boldsymbol{\theta}) = \frac{1}{2}(\boldsymbol{\theta} - \boldsymbol{\theta}^n)^T\mathcal{H}(\boldsymbol{\theta}^n)(\boldsymbol{\theta} - \boldsymbol{\theta}^n) \quad (9)$$

uniquely defined by the values of the output-sensitivity functions at sample times t_k, which can be obtained by the numerical integration of the following state-space representation derived from the deriving of (1) in relation to $\boldsymbol{\theta}$:

$$SF(\theta):\begin{cases}\dot{\phi}(t,\boldsymbol{\theta}) = J_{x(f)}(t,\boldsymbol{\theta}).\phi(t,\boldsymbol{\theta}) + J_{\theta(f)}(t,\boldsymbol{\theta})\\ \psi(t,\boldsymbol{\theta}) = J_{x(g)}(t,\boldsymbol{\theta}).\dot{\phi}(t,\boldsymbol{\theta}) + J_{\theta(g)}(t,\boldsymbol{\theta})\end{cases} \quad (10)$$

where $J_{x(f)} = \left[df_i/dx_j\right]$and $J_{x(g)}$ are the jacobian matrices of the function $\boldsymbol{f}$ and g in relation to $\boldsymbol{x}$, $J_{\theta(f)}$ and $J_{\theta(g)}$ are the jacobian matrices of $\boldsymbol{f}$ and g in relation to $\boldsymbol{\theta}$, and the state-matrix $\phi(t,\boldsymbol{\theta}) = \left[dx_i(t,\boldsymbol{\theta})/d\theta_j\right]$ contains the state-sensitivity functions. In other words, the identification of any model structure by the proposed method only requires the user to provide the analytical expression of the state-space functions $\boldsymbol{f}$ and g, and their four jacobians. These analytical functions can then be employed by a master function which ensures the numerical integration of (1) and (10), and the optimization of the quadratic criterion as proposed by (6).

D. Evaluation of the estimated parameter uncertainty

Near the optimum, the quadratic criterion (2) for the output error model can be re-arranged as follow:

$$D(\boldsymbol{\theta}) = \underbrace{\sum_{k=1}^{N} b(k)^2}_{E_n} + \underbrace{2\sum_{k=1}^{N} b(k)\left(y_m(k,\boldsymbol{\theta}_o) - y_m(k,\boldsymbol{\theta})\right)}_{Deformation} + \underbrace{\sum_{k=1}^{N}\left(y_m(k,\boldsymbol{\theta}_o) - y_m(k,\boldsymbol{\theta})\right)^2}_{S_{\boldsymbol{\theta}_o}(\boldsymbol{\theta})} \quad (11)$$

where $E_n = \sum_{k=1}^{N} b(k)^2$ is the energy of the noise that the optimization algorithm (6) should ideally reach. But as illustrated by Fig. 6, the second term of (11) deforms the hyper-ellipsoid $S_{\boldsymbol{\theta}^*}(\boldsymbol{\theta})$ defined by "true" value $\boldsymbol{\theta}^*$ of the parameter vector, and therefore the objective point $\boldsymbol{\theta}_o$ can be reached with $D(\boldsymbol{\theta}_o) < E_n$. This explains why the real objective of the identification should rather be to find the elliptic hyper-curve $C(\boldsymbol{\theta}_o, \alpha)$ given by the implicit equation $D(\boldsymbol{\theta}) = D_{min}(1+\alpha)$, where the coefficient α is chosen to ensure that $\boldsymbol{\theta}^*$ is inside the

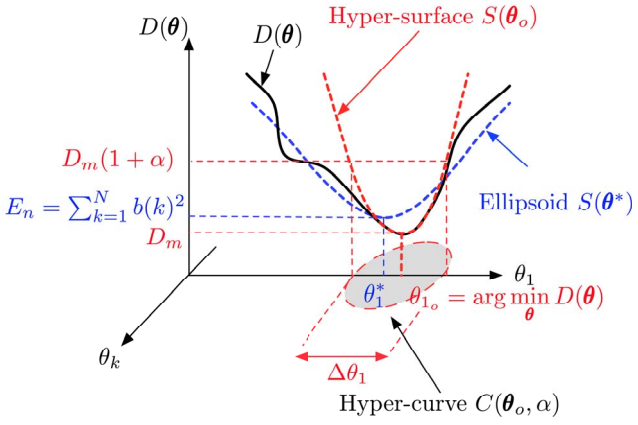

Fig. 6. Shape of the hypersurface criterion near the optimum.

iso-distance curve $C(\boldsymbol{\theta_o}, \alpha)$. If the output error $b(k)$ can be modeled by a random noise with normal distribution $\mathcal{N}(0, \sigma^2)$, then taking $\alpha_o = (9/N)$ allows to say that $\boldsymbol{\theta}^*$ has a probability of 95% to be inside $C(\boldsymbol{\theta_o}, \alpha_o)$ [25]. In more general case, one can only propose the smallest value which ensures that the intersection of iso-distance $C_m(\boldsymbol{\theta}, \alpha_o)$ obtained for different excitation protocols is not void.

Finally, the iteration algorithm (6) and the numerical integration of the sensitivity function state-space (10) give an approximation of the hessian matrix $\mathcal{H}(\boldsymbol{\theta_o})$, which analysis can reveal a valley in the hypersurface $S_{\boldsymbol{\theta}_0}(\boldsymbol{\theta})$. The presence of a valley in one parameter direction means that this parameter has not been sensibilized by the exication protocol. In fact, the condtion number (or eigenvalues) provide us information about the parameter uncertainties. For example, in the case of a two-dimension parametric space, the iso-distance curve $C(\boldsymbol{\theta_o}, \alpha)$ is an ellipse which equation in the eigenbase is given by:

$$\theta_1'^2.\lambda_1 + \theta_2'^2.\lambda_2 = \alpha D_{min} \tag{12}$$

where λ_1 and λ_2 are the eigenvalues of $\mathcal{H}(\boldsymbol{\theta_o})$. One can observe that the major and minor axis of $C(\boldsymbol{\theta_o}, \alpha)$ are inversely related to the square root of the eigenvalue values (Fig. 7). The parameters uncertainties $\Delta\theta_1$ and $\Delta\theta_2$ can thus be derived from the projection of the ellipse major and minor axis on the axes of the natural parametric space.

E. *Design of the optimal excitation protocol*

Let us note $\boldsymbol{\theta}_d = [\theta_1, \ldots, \theta_d]^T$ the d parameters concerned by the design of the diagnostic indicator, $DI(\boldsymbol{\theta}_d)$ the diagnostic indicator used for insulation diagnosis, and $\boldsymbol{p}$ the set of parameters that characterize the system excitation protocol. For a simple voltage step, it can be the length N of the records and its step amplitude. Then, as shown by Fig. 8, the optimal protocol parameter $\boldsymbol{p_o}$ for a given model structure can be obtained by the minimization of the diagnostic indicator uncertainty ΔDI, which expression is given by the law of uncertainty propagation:

$$\Delta DI(\boldsymbol{p}) = \sqrt{\sum_{k=1}^{d} \left(\frac{\partial DI}{\partial \theta_k}\right)^2 \Delta\theta_k(\boldsymbol{p}, \alpha_o)^2} \tag{13}$$

For each value of $\boldsymbol{p}$, the identification of the optimal parameters $\boldsymbol{\theta}_{d_o}$ and the evaluation of their uncertainty

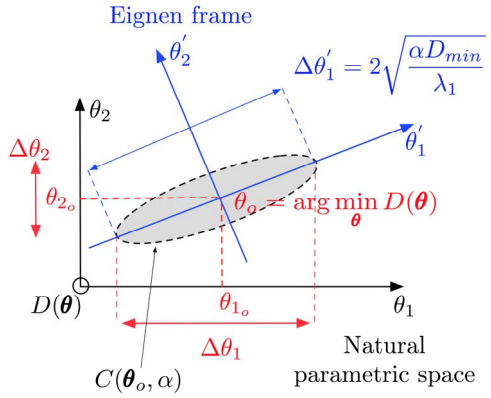

Fig. 7. Evaluation of the parameter uncertaincy.

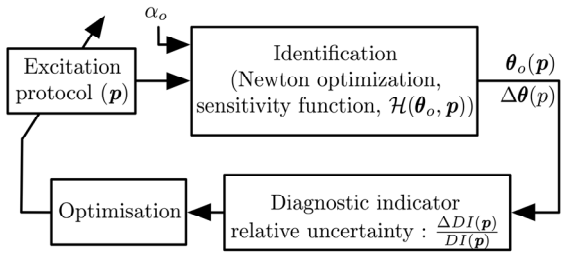

Fig. 8. Scheme of the protocol optimization.

$\Delta\theta_k(\boldsymbol{p}, \alpha_o)$ are determined using the above identification process.

F. *Identification in practice*

In practice, the protocol optimization is performed with a state distance normalized by the system output variance:

$$D_n(\boldsymbol{\theta}) = \frac{1}{N}\sum_{k=1}^{N} \boldsymbol{e}(k, \boldsymbol{\theta})^T W \boldsymbol{e}(k, \boldsymbol{\theta}) \tag{14}$$

where $W = 1/Var(y_s)$ if the system output is scalar (or a diagonal matrix in case of a multiple output system). $D_n(\boldsymbol{\theta})$ is therefore an a-dimensional normalized critrerion that allows not only to compare different protocols for a same model structure, but also to compare different model structures.

Moreover, the inversion of the hessian matrix may face to numerical problems when model parameters are in very different orders of magnitude. The solution consist in making the optimization (6) in the relative parametric space by the following variable change: $\delta\boldsymbol{\theta} = \mathrm{diag}(\boldsymbol{\theta_o}).\delta_r\boldsymbol{\theta}$, where $\delta_r\boldsymbol{\theta}$ is the relative variation of $\boldsymbol{\theta}$ near the optimum. By this way, the equation (9) of the hyperellispoïd around the optimum becomes:

$$S(\delta_r\boldsymbol{\theta}) = \delta_r\boldsymbol{\theta}^T \underbrace{\left(\mathrm{diag}(\boldsymbol{\theta_o}).\mathcal{H}(\boldsymbol{\theta_o}).\mathrm{diag}(\boldsymbol{\theta_o})\right)}_{\mathcal{H}_r(\boldsymbol{\theta_o})} \delta_r\boldsymbol{\theta}$$

and the optimization is then performed in a a-dimensional space, with a much better conditioned hessian matrix $\mathcal{H}_r(\boldsymbol{\theta_o})$.

III. Application with Experimental Data

For simplicity, the following illustrates the methodology with the identification of a simple lumped parameter model derived from the visual analysis of the current charging / discharging the winding insulation, and for the optimization of a step voltage excitation protocol.

A. *Experimental bench and measurements*

Fig. 9 presents the laboratory bench used for the experiments. The insulation system under test concerns a 1.5 kW delta connected induction motor. The excitation voltage is applied between one phase and the magnetic core. Fig. 10 shows the experimentl measurements used for identification: the input volatge $u = V_2(t)$ and the output $V_1(t) - V_2(t) = R_m i$ are defned by Fig. 4. Note that similar currents are obtained with a star connected machine, and also for the three phases.

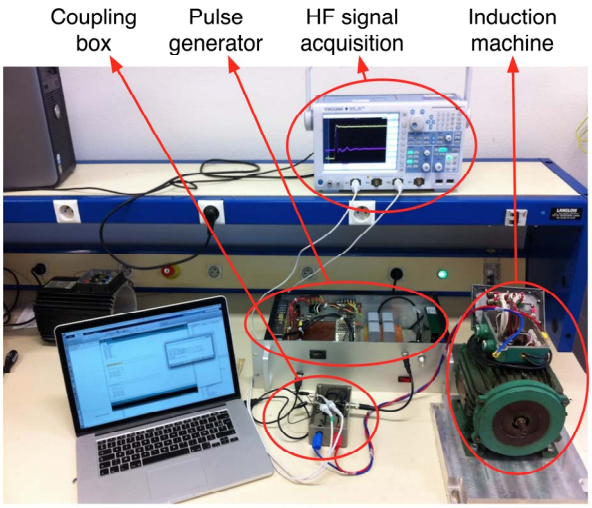

Fig. 9. Experimental bench.

B. Model identification

The parametric model proposed by Fig. 11 explains the shape of the measured current as the sum of three currents : $i = i_p + i_c + i_L$. Its justification in not in the scope of thisarticle. The function $\boldsymbol{f}$ and g of the state-space representation (1) are obtained considering the capacitance voltages and the inductance currents as state variables. Their analytical jacobian matrices can be obtained manually or with symbolic calculations. The parameters are first identified with the output error method coupled with the Nelder-Meder optimization algorithm. Then, the results can be used to initialize the Newton iteration algorithm (6). Fig 12 shows the good agreement between the measured and simulated currents for the estimated parameters and Table I gives the parameter means and standard deviations for ten experimental records.

TABLE I. ESTIMATED VALUES OF THE MODEL PARAMETERS

	$l\ (\mu H)$	R_p	R_c	$C\ (nF)$	R_L	$L\ ((\mu H)$	$C_L\ (nF)$
Mean	1	1800	19.5	0.350	101.2	15.3	0.159
Std	0.1	1	0.3	0.004	1.1	0.4	0.004

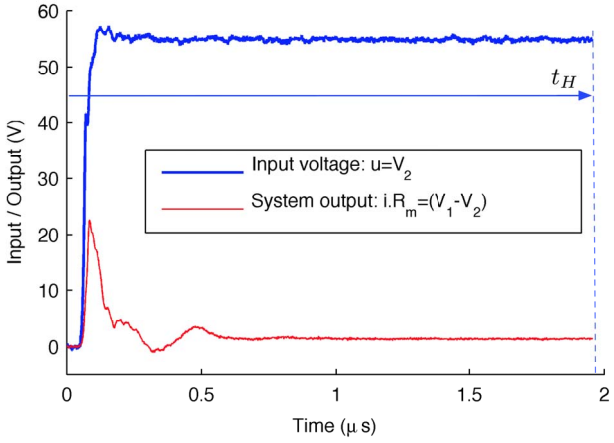

Fig. 10. Experimental measurement for a step excitation protocol

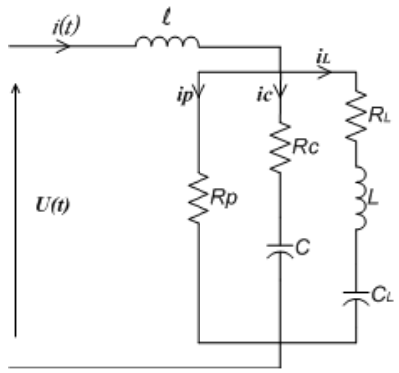

Fig. 11. The proposed model structure of the insulation system

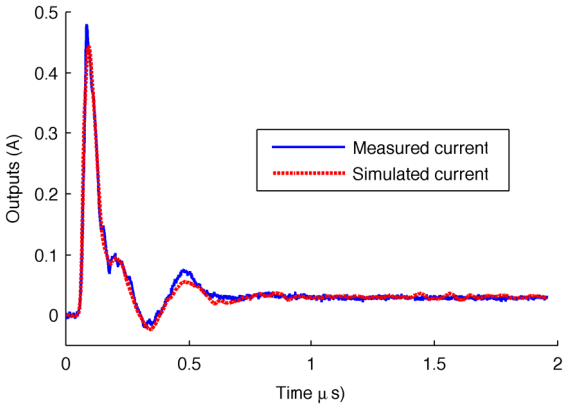

Fig. 12. Comparison bewteen measured and simulated currents

C. Protocol optimization

For the simplicity of explanations, we propose now to illustrate the methodology by optimizing the horizon t_H of the exciation protocol, for the previous model (see Fig. 10). Morever, let us suppose (even it is not exactly the case) that only the capacitance parameters C and C_L change with the insulation aging and that the diagnostic indicator to monitor is given by the ratio $DI = C/C_L$. Then, the relative uncertainty of this indicator is obtained thanks to (13):

$$\frac{\Delta DI}{DI} = \sqrt{\frac{\Delta C^2}{C^2} + \frac{\Delta {C_L}^2}{{C_L}^2}} \tag{15}$$

where the parameter uncertainties ΔC and ΔC_L depend on the choice of α and the lenght t_H of the records. Fig. 13 shows the evolution of this relative uncertainty. An optimal length of the step protocol is obtained for $t_H = 0.4$ µs.

IV. CONCLUSION

This study investigates the condition monitoring of the electrical machine insulation system for its predictive maintenance. The state monitoring is based on the in-situ identification of high frequency continuous-time models, by the output error method. The identification procedure takes the advantages of the numerical integration of the state-sensitivity functions for estimating the model parameters and their relative

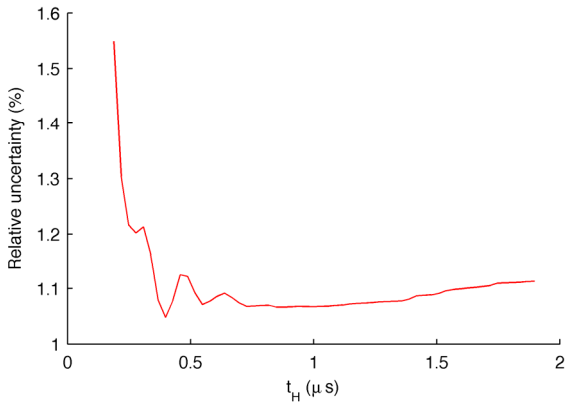

Fig. 12. Evolution of the Diagnostic Indicator relative uncertainty $\Delta DI/DI$ in respect to the length of the excitation protocol

uncertainty. Therefore, it provides an convenient way for finding the excitation protocol which offers the smallest uncertainty of the diagnostic indicator. The theoretical framework of the identification and the research of a structure model dedicated to insulation diagnosis is detailed and illustrated with a very simple model structure and with experimental data recorded from the stator winding of a standard 1.5 kW induction machine.

Now, with the developed experimental tools and the programed identification algorithms, it becomes very simple to analyze different continuous-time model structures. Future works will therefore explore the ability of complex structures derived from the *R-L-C* network modeling of winding insulation. And an industrial induction machine will be aged in accordance with IEEE standard aging procedures. This will allows to propose efficent aging indicators.

REFERENCES

[1] M. Muhr, « Aging and degradation, their detection and monitoring & asset management », in International Symposium on Electrical Insulating Materials, 2008. (ISEIM 2008), 2008, p. 183‑186.

[2] T. Judendorfer, J. Fletcher, N. Hassanain, M. Mueller, et M. Muhr, « Challenges to machine windings used in electrical generators in wave and tidal power plants », in IEEE Conference on Electrical Insulation and Dielectric Phenomena, 2009. CEIDP '09, 2009, p. 238‑241.

[3] World Energy Council 2013, « World Energy Resources: Marine Energy », www.worldenergy.org/, 2013. [Online]. Avialable on: http://www.worldenergy.org/publications/. [Consulted : April, 4th 2014].

[4] J. Yang, T. Kang, B. Kim, S.-B. Lee, Y.-W. Yoon, D. Kang, J. Cho, et H. Kim, « Experimental evaluation of using the surge PD test as a predictive maintenance tool for monitoring turn insulation quality in random wound AC motor stator windings », IEEE Trans. Dielectr. Electr. Insul., vol. 19, no 1, p. 53‑60, 2012.

[5] G. C. Stone, E. A. Boulter, I. Culbert, et H. Dhirani, Electrical insulation for rotating machines. Design, Evaluation, Aging, Testing and repair, IEEE press series on power engineering vol. 2003.

[6] G. C. Stone, « Recent important changes in IEEE motor and generator winding insulation diagnostic testing standards », IEEE Trans. Ind. Appl., vol. 41, no 1, p. 91‑100, 2005.

[7] S. B. Lee, K. Younsi, et G. B. Kliman, « An online technique for monitoring the insulation condition of AC machine stator windings », IEEE Trans. Energy Convers., vol. 20, no 4, p. 737 ‑ 745, déc. 2005.

[8] F. Perisse, P. Werynski, et D. Roger, « A New Method for AC Machine Turn Insulation Diagnostic Based on High Frequency Resonances », IEEE Trans. Dielectr. Electr. Insul., vol. 14, no 5, p. 1308‑1315, October.

[9] W. Liu, E. Schaeffer, D. Averty, et L. Loron, « A new Approach for Electrical Machine Winding Insulation Monitoring by Means of High Frequency Parametric modelling », in IECON 2006 - 32nd Annual Conference on IEEE Industrial Electronics, Nov., p. 5046‑5050.

[10] W. Liu, E. Schaeffer, L. Loron, et P. Chanemouga, « High Frequency Modelling of Stator Windings Dedicated to Machine Insulation Diagnosis by Parametric Identification », in IEEE International Symposium on Diagnostics for Electric Machines, Power Electronics and Drives, 2007. SDEMPED 2007, Sept., p. 480‑485.

[11] F. Perisse, D. Mercier, E. Lefevre, et D. Roger, « Robust diagnostics of stator insulation based on high frequency resonances measurements », IEEE Trans. Dielectr. Electr. Insul., vol. 16, no 5, p. 1496‑1502, October.

[12] J.-C. Trigeassou, Diagnostic des machines électriques. Hermes Science Publications, 2011.

[13] R. Toscano, « Commande et diagnostic des systèmes dynamiques, modélisation, analyse, commande par PID et par retour d'état, diagnostic », ellipses, 2005.

[14] M. T. Wright, S. J. Yang, et K. McLeay, « General theory of fast-fronted interturn voltage distribution in electrical machine windings », Electr. Power Appl. IEE Proc. B, vol. 130, no 4, p. 245‑256, juill. 1983.

[15] J. L. Guardado, J. A. Flores, V. Venegas, J. L. Naredo, et F. A. Uribe, « A machine winding model for switching transient studies using network synthesis », IEEE Trans. Energy Convers., vol. 20, no 2, p. 322‑328, juin 2005.

[16] V. Venegas, J. L. Guardado, E. Melgoza, et M. Hernandez, « A Finite Element Approach for the Calculation of Electrical Machine Parameters at High Frequencies », in IEEE Power Engineering Society General Meeting, 2007, 2007, p. 1‑5.

[17] J.-C. Trigeassou, Electrical Machines Diagnosis. John Wiley & Sons, 2013.

[18] P. Eykhoff, System identification: parameter and state estimation. Wiley-Interscience, 1974.

[19] L. Ljung, System Identification: Theory for the User. Pearson Education, 1998.

[20] É. Walter et L. Pronzato, Identification of parametric models from experimental data. Springer, 1997.

[21] J.-C. Trigeassou, T. Poinot, et S. Bachir, Parameter estimation for knowledge and diagnosis of electrical machines. HAL□: hal-00782890, version 1, Control Methods for Electrical Machines, ISTE Ltd and John Wiley & Sons Inc (Ed.). 2013.

[22] J.-C. Trigeassou, Recherche de modèles expérimentaux assistés par ordinateur. Paris: Tec&Doc,LAVOISIER, 1988.

[23] D. M. Olsson et L. S. Nelson, « The Nelder-Mead Simplex Procedure for Function Minimization », Technometrics, vol. 17, no 1, p. 45‑51, 1975.

[24] S. Bachir, S. Tnani, J.-C. Trigeassou, et G. Champenois, « Diagnosis by parameter estimation of stator and rotor faults occurring in induction machines », IEEE Trans. Ind. Electron., vol. 53, no 3, p. 963 ‑ 973, juin 2006.

[25] J. Richalet, A. J. Rault, et R. Pouliquen, Identification des processus par la méthode du modèle. Gordon & Breach, 1971.